

Vibronic structure, energy level, and incorporation mechanism of Ti^{3+} in LiNbO_3 and LiTaO_3

O. Thiemann, H. Donnerberg, M. Wöhlecke, and O.F. Schirmer

Department of Physics, University of Osnabrück, P. O. Box 4469, D-49069 Osnabrück, Federal Republic of Germany

(Received 21 May 1993; revised manuscript received 10 November 1993)

In reduced LiTaO_3 , an axially symmetric EPR signal with $g_{\parallel} = 1.948 \pm 0.003$ and $g_{\perp} = 1.827 \pm 0.003$ has been identified. It is attributed to Ti^{3+} ($3d^1$) by comparison with the already known EPR data of Ti^{3+} in LiNbO_3 . We are able to explain the g values of this center in LiNbO_3 as well as in LiTaO_3 , by a model calculation involving a dynamic pseudo Jahn-Teller effect. Spin-orbit coupling, lattice vibration, pseudo Jahn-Teller interaction, and the Zeeman term are treated on equal footing. Intervalence transfer from Ti^{3+} to Nb^{5+} , forming a $\text{Nb}_{\text{Li}}^{4+}$ polaron, has been identified. This transfer can be stimulated either by visible light or by thermal activation. By investigating the temperature dependence of the thermally activated intervalence transfer, we have determined the ionization energy of Ti^{3+} with respect to $\text{Nb}_{\text{Li}}^{4+}$ to be $0.11 \text{ eV} \pm 0.02 \text{ eV}$.

I. INTRODUCTION

The optical applications of lithium niobate are determined to a large extent by intrinsic and extrinsic defects. For instance, iron plays a key role in sensitizing the material for photorefractive applications. Titanium is used for producing optical waveguides in LiNbO_3 crystals. By indiffusion of Ti into the outer layers of the material the refractive index is increased, allowing to shape the way of light propagation. The present paper reports a continuation of research into the microscopic properties of Ti in LiNbO_3 , which we had started with the aim to eventually explain why Ti doping increases the refractive index.

Previously we identified Ti^{3+} in chemically reduced LiNbO_3 by EPR.^{1,2} The resonance is described by an axial g tensor, $g_{\perp} = 1.964$ and $g_{\parallel} = 1.840$, consistent with the C_3 symmetry expected for isolated Ti on a cation site of the lattice. The proximity of the g values to 2 points to a nondegenerate Γ_1 ground state. There are indications, to be presented below, that the magnetic properties of this state are influenced by vibronic coupling. We shall show that taking into account pseudo Jahn-Teller interaction can qualitatively explain the vibronic effects on the ground state Zeeman splitting.

The position of defect energy levels is unknown for most centers in oxide crystals, especially LiNbO_3 . By analysis of the temperature dependence of the optical absorption spectra of $\text{Ni}_{\text{Li}}^{4+}$ and Ti^{3+} in LiNbO_3 we shall demonstrate that the $\text{Ti}^{3+/4+}$ level lies slightly below $\text{Nb}_{\text{Li}}^{4+/5+}$.

Before treating these issues connected with LiNbO_3 the EPR identification of Ti^{3+} in the isomorphous LiTaO_3 will be reported. In the following section we describe the influence of vibronic interaction on the ground states of Ti^{3+} in LiNbO_3 and LiTaO_3 . Finally, the determination of the ionization energy of Ti^{3+} will be reported and discussed.

II. EXPERIMENT

The reduction treatment, the EPR measurements and the optical absorption spectra have been performed with nominally pure, LiTaO_3 and Ti-doped LiNbO_3 . The first was purchased from Union Carbide Crystal Products, while the latter, with 1 mol % Ti in the melt, was kindly supplied by the Siemens Crystal Growth Laboratory in Munich. The effective distribution coefficient of Ti^{4+} in LiNbO_3 is given by Räufer³ to be 0.8. Thus the Ti content in the crystal should be about 0.8 mol %.

For the reduction treatment we used a horizontally mounted quartz tube heatable with an oven up to 1400 K. Both evacuation or the setup of a continuous gas flow was possible. In the case of LiTaO_3 we reduced the sample at 1300 K for 15 h in a H_2 atmosphere. The LiNbO_3 :Ti sample was strongly reduced at 1300 K in vacuum of about 2×10^{-5} mbar for several hours.

The g values of the centers in both samples have been measured with a conventional Bruker ER 200 D-SRC spectrometer working in the X band at temperatures down to 15 K. For the optical absorption measurements we used a Beckman Acta MVII spectrometer equipped with a suitable cryostat for low temperatures (10–380 K) and an oven for high ones (293–1073 K). In order to prevent reoxidation at elevated temperatures, the crystal was kept in a heatable transmission cell in an argon atmosphere during the experiment. We were sure that no further reduction took place, because no additional coloration could be observed by comparing the absorption before and after the heating cycle. For high temperatures a nonstandard operation mode with the spectrometer between the sample and the detector was used. This allows one to block the strong Planck radiation emitted from a crystal at elevated temperatures.

III. EPR OF Ti^{3+} IN LiTaO_3

In the reduced, nominally pure, LiTaO_3 crystal, we observed an EPR signal of axial symmetry at a temper-

ature of about 15 K with $g_{\parallel} = 1.948 \pm 0.003$ and $g_{\perp} = 1.827 \pm 0.003$. The g values are similar to those established for Ti^{3+} in LiNbO_3 : $g_{\parallel} = 1.964$ and $g_{\perp} = 1.840$. The almost quantitative agreement suggests the assignment of the newly found signal to Ti^{3+} in LiTaO_3 . The large linewidths, 35 mT and 45 mT for $\mathbf{B} \parallel \mathbf{c}$ and $\mathbf{B} \perp \mathbf{c}$, respectively, precluded the identification of a hyperfine interaction due to the low abundant magnetic isotopes ^{47}Ti ($I = 5/2$) and ^{49}Ti ($I = 7/2$).

In contrast to LiNbO_3 where Ti replaces the Li ion⁴ it is not yet established whether Ti replaces Li or Ta in LiTaO_3 . Nevertheless the site symmetry of both cations is C_3 . Therefore also in LiTaO_3 we expect a g tensor of axial symmetry, which agrees with the experimental data obtained. Again the g tensor can only be explained by a nondegenerate Γ_1 orbital ground state (site symmetry C_3), which is separated by the trigonal field splitting Δ from the excited Γ_2, Γ_3 (C_3) states. Following Abragam and Bleaney,⁵ one obtains

$$\begin{aligned} g_{\parallel} &= g_s \cos 2\theta - k(1 - \cos 2\theta), \\ g_{\perp} &= \frac{1}{2}g_s(1 + \cos 2\theta) - \sqrt{2}k \sin 2\theta, \end{aligned} \quad (1)$$

using an isotropic orbital reduction factor $k = k_{\parallel} = k_{\perp}$. Before we discuss the parameter θ we note that such orbital reduction factors are commonly used to account for covalency effects within a static crystal field description. More accurately, they describe the changes of matrix elements of the angular momentum operator L , when atom-like orbitals $|d_i\rangle$ are used instead of molecular orbitals $|\phi_i\rangle$.⁵

$$\langle \phi_n | L | \phi_m \rangle = k_{nm} \langle d_n | L | d_m \rangle.$$

Spin-orbit interaction is given accordingly by

$$\begin{aligned} \langle \phi_n | \lambda_{nm} \mathbf{L} \cdot \mathbf{S} | \phi_m \rangle &= \lambda_{nm} k_{nm} \langle d_n | \mathbf{L} \cdot \mathbf{S} | d_m \rangle \\ &= \lambda_0 r_{nm} k_{nm} \langle d_n | \mathbf{L} \cdot \mathbf{S} | d_m \rangle. \end{aligned}$$

Here $r_{nm} = \lambda_{nm}/\lambda_0$ takes into account the change of the free-ion spin-orbit coupling constant in a crystalline environment. The parameter θ [$\tan 2\theta = \sqrt{2}\lambda/(\Delta + \lambda/2)$] depends on the spin-orbit coupling parameter λ and the trigonal crystal field splitting Δ , while $g_s = 2.0023$ is the free spin value. The evaluation of the experimental g values of Ti^{3+} in LiTaO_3 and in LiNbO_3 on the basis of these expressions leads to unusually low k values, $k < 0.6$ (see Table I). On the other hand in oxides the lower bound of the orbital reduction factors, due to covalent admixture of ligand orbitals to the wave function of the central ion, is generally expected to be about 0.7.⁶ Since it is known that electron-phonon coupling can lead to orbital reduction factors smaller than those due to covalency only, we studied the influence of this interaction as an additional contribution.

IV. PSEUDO JAHN-TELLER TREATMENT OF THE ZEEMAN EFFECT OF THE Ti^{3+} GROUND STATE

We obtained axial g tensors for Ti^{3+} in both LiNbO_3 and LiTaO_3 . The site symmetry of Ti^{3+} in these compounds is C_3 , but the deviation from C_{3v} is small. It consists only in a small rotation of the corners of the oxygen triangles out of the vertical mirror planes. Therefore we shall assume C_{3v} site symmetry in the following treatment, which is based on symmetry arguments. The ground state of Ti^{3+} in cubic symmetry is ${}^2T_{2g}(\Gamma_5)$. Lowering the symmetry to C_{3v} results in an orbital singlet ground state Γ_1 and an excited doublet state Γ_3 .

In the similar case of Ti^{3+} in Al_2O_3 the sign of the axial crystal field causes the orbital doublet to lie lowest. Thus a dynamic Jahn-Teller effect could be invoked to explain the EPR properties of the $\text{Al}_2\text{O}_3:\text{Ti}^{3+}$ system.⁷ For Ti^{3+} in LiNbO_3 and LiTaO_3 the axial crystal field has the opposite sign, and the ground state is the orbital singlet. Therefore a dynamic *pseudo* Jahn-Teller mechanism will be introduced, using a vibronic coupling between the singlet ground state and the doublet excited state. We consider vibrational coupling only among the Γ_1 and Γ_3 orbital states arising from the cubic ${}^2T_{2g}$ ground state of Ti^{3+} because of the large cubic field splitting 10 Dq of about 20 000 cm^{-1} . The Hamiltonian is given by

$$H = H_{\text{CF}}(C_{3v}) + H_{\text{SO}} + H_{\text{vib}} + H_{\text{JT}} + H_{\text{Zee}} \quad (2)$$

in self-evident notation. In finding the eigenvalues of this Hamiltonian we shall treat the spin-orbit coupling, the trigonal crystal field, the vibration, the Jahn-Teller coupling, and the Zeeman term on equal footing. A similar calculation has first been performed by Ham *et al.*⁸

Different to our approach Bates *et al.*⁹ and Macfarlane *et al.*⁷ used in their corresponding investigation of $\text{Al}_2\text{O}_3:\text{Ti}^{3+}$ a perturbation treatment, where trigonal crystal field, spin-orbit interaction, and the Zeeman term are considered as being perturbations with respect to the leading terms

$$H_0 = H_{\text{CF}}(O_h) + H_{\text{vib}} + H_{\text{JT}} \quad (3)$$

in the total Hamiltonian. These perturbation approaches allow one to include an infinite number of JT-active phonons. However, we feel that a perturbation expansion to second order is not appropriate for Ti^{3+} in LiNbO_3 , LiTaO_3 , and Al_2O_3 : First- and second-order contributions to the perturbation matrix are seen to be of the same order of magnitude. Thus one cannot draw any proper conclusions regarding the quality and even the *existence* of convergence^[10–12]. Similar observations have been made by Rai.¹³ Alternatively Rai suggested a per-

TABLE I. EPR parameters of Ti^{3+} in LiNbO_3 and LiTaO_3 .

	g_{\parallel}	g_{\perp}	δ	λ/Δ	k	Ref.
$\text{LiNbO}_3:\text{Ti}^{3+}$	1.964	1.840	0.029π	0.14	0.58	[Juppe (Ref. 1), Müller (Ref. 2)]
$\text{LiTaO}_3:\text{Ti}^{3+}$	1.948	1.827	0.033π	0.14	0.52	(This work)

turbation treatment of parts of the JT effect (i.e., the tunneling) assuming that covalency is negligible. However, also in this case the validity of perturbation theory is not obvious, as the results of Rai indicate a dominating dynamic behavior. Moreover, we refer in this context to a paper by Pryce,¹⁴ where the importance of covalency effects has been emphasized.

These few comments may suffice to justify our different approach. However, we should also note that in our treatment, although avoiding any perturbation calculations, principally only a limited number of phonons can be included (otherwise the size of the Hamiltonian matrix is increasing rapidly with each additional phonon). In conclusion we believe our treatment is necessary to support the idea of dynamic Jahn-Teller effects for Ti^{3+} ions embedded in trigonally distorted crystals.

The trigonal field splitting is described by the parameter Δ . The spin-orbit term removes the orbital degeneracy of Γ_3 , which results in the irreducible representations $\Gamma_4, \Gamma_5, \Gamma_6$ of the C_{3v} double group, using the notation of Koster *et al.*¹⁵ For admixing the electronic excited orbital state Γ_3 to the ground state Γ_1 by pseudo Jahn-Teller coupling, phonons of E symmetry (in C_{3v}) have to be used. In C_{3v} there exist the two (degenerate) normal vibrations Q_x and Q_y having E symmetry. The vibrational basis functions Q_e and Q_θ , which transform like $-S_+$ and S_- in the notation of Koster *et al.*,¹⁵ do not represent normal vibrations. The operators corresponding to Q_e and Q_θ are not Hermitian, but can be expressed by a linear combination of the Hermitian operators Q_x and Q_y :

$$Q_e = \frac{1}{\sqrt{2}}(Q_x - iQ_y) = \frac{a}{\sqrt{2}}(X^+ + Y),$$

$$Q_\theta = \frac{1}{\sqrt{2}}(Q_x + iQ_y) = \frac{a}{\sqrt{2}}(X + Y^+),$$

where $a = \sqrt{\hbar/m\omega}$ and $X^+, Y^+, X,$ and Y are the up and down leiteroperators related to Q_x and Q_y , respectively.

From the coupling coefficients of C_{3v} the Jahn-Teller Hamiltonian is deduced:

$$H_{\text{JT}} = V(E_e Q_\theta + E_\theta Q_e), \quad (4)$$

where V is the reduced matrix element of the tensoroperators $E_{e,\theta}$, which are operating on the electronic wave functions $|\xi\rangle, |\eta\rangle,$ and $|\zeta\rangle$. The coupling strength described by the reduced matrix element V is considered to be equal for simplicity for $\Gamma_3 \otimes \Gamma_3$ and $\Gamma_1 \otimes \Gamma_3$. The equidistant energy levels of the E vibration are shown in Fig. 1. The spin-orbit coupling is treated as being spherically symmetric ($H_{\text{SO}} \sim \mathbf{L} \cdot \mathbf{S}$) and the orbital reduction factor k as being isotropic.

The symmetry adapted vibronic basis set is obtained by coupling the E mode vibration to the spin-orbit states $\Gamma_4, \Gamma_5,$ and Γ_6 , considering phonons up to a quantum number of $n_E = n_e + n_\theta = 2$. This yields 36 basis states having symmetry $\Gamma_4, \Gamma_5,$ and Γ_6 . The total Hamiltonian was expressed in matrix form by this new vibronic basis set. The energy eigenvalues of this 36×36 matrix were obtained by numerical diagonalization.

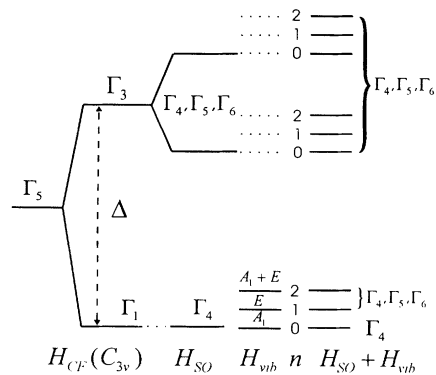


FIG. 1. Energy level scheme resulting from the Γ_5 (${}^2T_{2g}$) ground state of Ti^{3+} in cubic symmetry. For details refer to the discussion in the text.

Using this procedure, reasonable parameter values reproducing the experimental g tensor components can be chosen; these parameters are the covalent orbital reduction factor k , the parameter $\delta = \lambda/\Delta$ (where λ describes the reduced spin-orbit coupling constant in the crystalline environment), the Jahn-Teller energy E_{JT} ($E_{\text{JT}} = V^2/2m\omega^2$), and the phonon energy $\hbar\omega$ of the coupled vibration mode. Such choices are not possible if electron-phonon interaction is not taken into account. In the moderately covalent Al_2O_3 , which has the same crystallographic structure as LiNbO_3 , the orbital reduction factor k for transition-metal ions has typically values between 0.7 and 0.8. For LiNbO_3 we therefore choose $k = 0.75$. The spin-orbit coupling parameter λ is taken to be 123 cm^{-1} , which is 80% of the free-ion value. This accounts for a reasonable expansion of the $3d$ radial function in the solid. The wave number of the interacting phonon was assumed to be $\tilde{\nu} = 258 \text{ cm}^{-1}$, which is the weighted mean of the LiNbO_3 phonon density of states, as measured by Raman scattering.¹⁶ By fitting the g values with the given parameters we obtained a Jahn-Teller energy of $E_{\text{JT}} = 319 \text{ cm}^{-1}$ and a trigonal crystal field splitting of $\Delta = 820 \text{ cm}^{-1}$. It was not yet possible to check this value of the crystal field splitting by optical absorption. In Al_2O_3 for comparison the trigonal crystal field splitting for several trivalent $3d^n$ ions is in the range $700\text{--}1000 \text{ cm}^{-1}$. The numbers listed above for the parameters $k, \delta, E_{\text{JT}},$ and $\tilde{\nu}$ are only representative values. Agreement can also be found within a wider range of parameter values. For a systematic investigation we varied k and $\tilde{\nu}$. The results are plotted in the parameter space δ vs E_{JT} in Fig. 2. For three different k values (0.7, 0.75, and 0.8) the obtained pairs of δ and E_{JT} are shown, which reproduce the experimental g values. In Fig. 2 also the effect of varying $\tilde{\nu}$ by $\pm 50 \text{ cm}^{-1}$ is indicated.

The obtained exact fit of the measured g values with the indicated model calculation can only be taken as a qualitative indication that vibronic interaction in the form of a pseudo Jahn-Teller effect can explain the puzzling observation that the effective k values for Ti^{3+} in LiNbO_3 are considerably smaller than the covalent reductions generally found for $3d$ ions in oxide materials. In this approach the number of phonons coupling to the

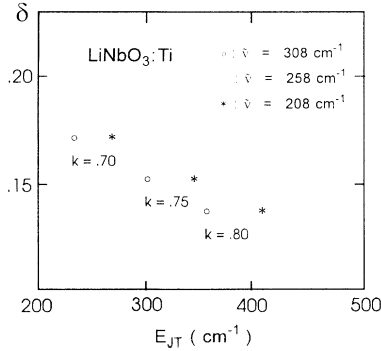


FIG. 2. Results of the pseudo Jahn-Teller calculation of the Zeeman effect of the Ti^{3+} ground state in LiNbO_3 . The experimental g values can be reproduced by the pairs of E_{JT} and $\delta = \lambda/\Delta$, which are represented by the given symbols. The symbols denote different assumed phonon energies. The range of the expected k values is indicated.

spin-orbit states had to be limited to two for technical reasons. In order to get an idea of the influence of the number of coupled phonons, the calculation was done for 0, 1, and 2 coupled phonons with the other parameters fixed. We found a decrease of the separation between the g -value pairs (g_{\parallel} , g_{\perp}) by increasing the phonon number. We cannot decide, however, whether the convergence obtained is sufficient to warrant more than a qualitative statement about the applicability of the model.

With the same procedure we were also able to explain the experimental g values of Ti^{3+} in LiTaO_3 using similar parameters. This is not surprising because of the related crystallographic and phonon structure.

V. OPTICAL AND THERMAL INTERVALENCE TRANSFER: $\text{Ti}^{3+} + \text{Nb}^{5+} \leftrightarrow \text{Ti}^{4+} + \text{Nb}^{4+}$

Illumination of a strongly reduced Ti-doped LiNbO_3 crystal at low temperatures gives rise to an intervalence transfer from Ti^{3+} to Nb^{5+} : $\text{Ti}^{3+} + \text{Nb}^{5+} \leftrightarrow \text{Ti}^{4+} + \text{Nb}^{4+}$. Here and in the following Nb is meant to designate a Nb_{Li} antisite defect; an electron bound at this site, Nb^{4+} , is stabilized to a large extent by lattice distortion and can thus be called a bound small polaron. Figure 3 shows the decrease of the Ti^{3+} and increase of the Nb^{4+} EPR signal after illumination with the unfiltered light of a 150 W xenon arc lamp at 20 K. At this low temperature Nb^{4+} is metastable. The indicated transfer is a special example of the photoionization of a $3d$ ion in LiNbO_3 , initiating the photorefractive effect. The details of the EPR spectrum are discussed elsewhere.¹⁷

We have also monitored the thermal ionization of Ti^{3+} . Since the EPR of Ti^{3+} and Nb^{4+} can only be detected up to about 100 K because of too short spin lattice relaxation times, we measured instead the temperature dependence of the intensities of the optical absorption bands of Ti^{3+} and Nb^{4+} . Similar investigations of the thermal dissociation of $\text{Nb}_{\text{Li}}^{4+}\text{-Nb}_{\text{Nb}}^{4+}$ bipolarons have been published previously.¹⁸

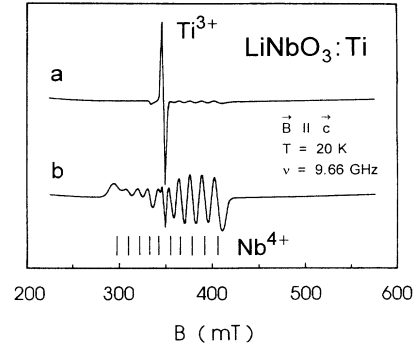


FIG. 3. The EPR spectra of Ti^{3+} and $\text{Nb}_{\text{Li}}^{4+}$ in $\text{LiNbO}_3\text{:Ti}$ indicating an optically induced intervalence transfer from Ti^{3+} to $\text{Nb}_{\text{Li}}^{5+}$ (a) before illumination, (b) after illumination.

By the strong reduction of the $\text{LiNbO}_3\text{:Ti}$ sample 0.3 mol % were changed into Ti^{3+} as monitored by EPR. After illuminating this reduced crystal only Nb^{4+} was observed by EPR beside the decreased Ti^{3+} signal. In the as-grown crystal no paramagnetic defects could be detected in EPR. Figure 4 shows the optical absorption of this crystal for $\mathbf{E} \parallel \mathbf{c}$ and its temperature dependence. At low temperatures a broad nearly unstructured band with peak at about 580 nm is extending over the whole visible and much of the near IR spectral range. This absorption decreases upon heating. Instead an additional absorption band with maximum around 760 nm rises. We note that the position of this maximum can be inferred without doubt by inspection of the corresponding absorption spectra at $T = 1073$ K (see inset of Fig. 4). The decrease of the initial absorption band at 580 nm must be due to an electronic transfer diminishing the concentration of the absorbing centers and cannot be ascribed to vibronic broadening because of two reasons: the zeroth

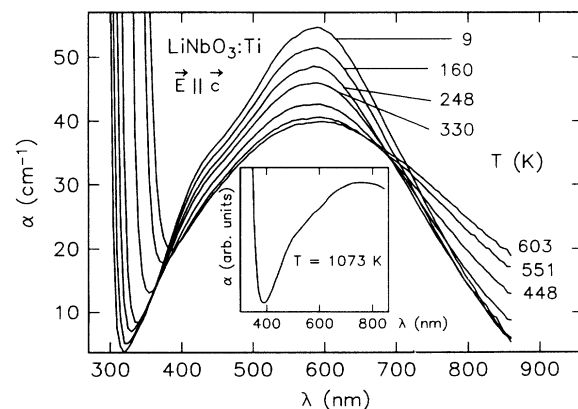


FIG. 4. Temperature dependence of the optical absorption of Ti-doped LiNbO_3 for a polarization $\mathbf{E} \parallel \mathbf{c}$. A strong absorption peaked at 760 nm grows with rising temperature, while the main absorption at 580 nm is decreasing. We explain this process as the thermally activated intervalence transfer $\text{Ti}^{3+} + \text{Nb}^{5+} \leftrightarrow \text{Ti}^{4+} + \text{Nb}^{4+}$. Inset: unpolarized optical absorption for a temperature of 1073 K.

moment of this absorption is really decreasing (this can directly be seen for temperatures below 250 K) and its first moment is nearly constant. At high temperatures ($T = 1073$ K) the band at 580 nm still exists beside the second one peaked at 760 nm.

The line shape of the total absorption is characteristic for each temperature and does not depend on the way the temperature is reached. This ascertains the increasing and decreasing absorption to be in a stationary equilibrium.

The absorption band at low temperatures with peak at 580 nm consists of six unresolved bands from which at least four are definitely assigned to Ti^{3+} . This was proved by ODMR (optically detected magnetic resonance) via MCD (magnetic circular dichroism, for a review see, e.g., Spaeth *et al.*¹⁹) as has been reported elsewhere (Thiemann *et al.*²⁰) The absorption peaked at 760 nm, which rises for $T \geq 250$ K, is attributed to the isolated $\text{Nb}_{\text{Li}}^{4+}$ polaron by comparing its position and line shape with that of the band first reported by Sweeney *et al.*,²¹ and correlated to $\text{Nb}_{\text{Li}}^{4+}$ by Dutt *et al.*²² It is obvious that the optical behavior mirrors the thermal intervalence transfer from the $\text{Ti}^{4+/3+}$ energy level to the $\text{Nb}^{5+/4+}$ level. It should be noted that the Ti ions are known to produce the highest energy levels within the gap of LiNbO_3 as compared with most other 3d ions (Thiemann *et al.*²³).

We shall now discuss the determination of the energy difference between the levels $\text{Ti}^{4+/3+}$ and $\text{Nb}^{5+/4+}$ as derived from the temperature dependence of the Nb^{4+} and Ti^{3+} absorption bands. The law of mass action of the considered intervalence transfer is given by

$$\frac{[\text{Ti}^{4+}] \cdot [\text{Nb}^{4+}]}{[\text{Ti}^{3+}] \cdot [\text{Nb}^{5+}]} = \exp(-\Delta E/k_B T) \exp(-\Delta S/k_B). \quad (5)$$

Since the degeneracies of the ground states of both Ti^{3+} and Nb^{4+} are identical, the entropy change of the transfer is zero: $\exp(-\Delta S/k_B) = 1$. The total initial Ti concentration, $[\text{Ti}]_0$, is assumed to be 0.8 mol %, see above. This includes both stable charge states of Ti, Ti^{3+} , and Ti^{4+} . For $[\text{Nb}]_0$ we take the concentration of the isolated Nb_{Li} antisite defects, 1.2 mol %, ²⁴ including both Nb^{5+} and Nb^{4+} ; the latter is responsible for the ten-line EPR in Fig. 3 and the optical absorption peaked at 760 nm, ^{25,26} Fig. 4. Assuming that Ti replaces the Nb_{Li} antisite, the effective initial $[\text{Nb}]_0$ may be lowered to 0.4 mol % (1.2 mol %, $[\text{Ti}]_0$). The initial concentrations of Nb^{4+} and Ti^{3+} are $[\text{Nb}^{4+}]_0 = 0$ and $[\text{Ti}^{3+}]_0 = 0.3$ mol %, as determined by EPR. Using these quantities Eq. (5) can be transcribed into

$$\frac{([\text{Ti}]_0 - [\text{Ti}^{3+}]_0 + [\text{Nb}^{4+}])([\text{Nb}^{4+}])}{([\text{Ti}^{3+}]_0 - [\text{Nb}^{4+}])([\text{Nb}]_0 - [\text{Nb}^{4+}])} = \exp(-\Delta E/k_B T). \quad (6)$$

Here $[\text{Nb}^{4+}]$ means the actual $\text{Nb}_{\text{Li}}^{4+}$ concentration, depending on temperature. $[\text{Nb}^{4+}]$ is created entirely from $[\text{Ti}^{3+}]$ and thus is equal to the vanished $[\text{Ti}^{3+}]$ or, alternatively, to the created $[\text{Ti}^{4+}]$. From Eq. (6) $[\text{Nb}^{4+}]$ can be calculated as depending on $\Delta E/k_B T$.

In Fig. 5 the logarithm of $[\text{Nb}^{4+}]$ is plotted vs the

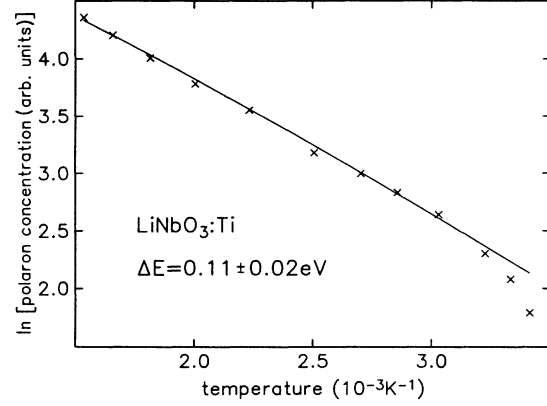


FIG. 5. Arrhenius plot of the polaron concentration. The ionization energy of $\Delta E = 0.11 \text{ eV} \pm 0.02 \text{ eV}$ for Ti^{3+} is given by the simulation (full line) of the high temperature range. The experimental values are indicated by \times .

reciprocal temperature $1/T$. $[\text{Nb}^{4+}]$ was determined from the absorption at 870 nm. The Ti^{3+} absorption at this wavelength is about 20% of the peak absorption at 580 nm. The total absorption is given by $C(\nu, T) = A(\nu)a(T) + B(\nu)b(T)$. Here $A(\nu)$ and $B(\nu)$ mean the Ti^{3+} and Nb^{4+} line shapes and $a(T)$, $b(T)$ are temperature dependent factors. In the following the temperature dependence of the width and the temperature shift of the maximum of the line shapes will be neglected. This is a good approximation as seen in Fig. 4.

The nearly linear range of the plot in Fig. 5 can be simulated very well by our simple model, using the above concentrations, with an ionization energy $\Delta E = 0.11 \text{ eV}$ (full line in Fig. 5). For low temperatures deviations from this linear behavior occur, which must be treated by a more complicated model. It should be noted that the obtained ionization energy, 0.11 eV, is rather insensitive to the assumed initial concentrations. Also $[\text{Nb}]_0 = 1.2$ mol %, valid if Ti does not replace Nb_{Li} , and a range of values for $[\text{Ti}^{3+}]_0$, all lead to $\Delta E = 0.11 \pm 0.02 \text{ eV}$, see Table II.

In reduced undoped LiNbO_3 generally a wide absorption band peaked near 500 nm is found which is attributed to $\text{Nb}_{\text{Li}}^{4+} - \text{Nb}_{\text{Nb}}^{4+}$ bipolarons.¹⁸ Also this band decreases by heating and again the absorption at 760 nm, due to $\text{Nb}_{\text{Li}}^{4+}$, rises. The underlying process was explained to be the thermal dissociation of bipolarons, leading to isolated $\text{Nb}_{\text{Li}}^{4+}$, the dissociation energy being $0.27 \pm 0.02 \text{ eV}$;¹⁸ i.e., the bipolaron stabilization energy per electron is similar to the ionization energy of Ti^{3+} . The overlap

TABLE II. Ionization energy ΔE for different initial parameters ($[\text{Ti}]_0 = 0.8$ mol %; $[\text{Nb}^{4+}]_0 = 0$ mol %).

$[\text{Ti}^{3+}]_0$ (mol %)	$[\text{Nb}]_0$ (mol %)	ΔE (eV)
0.1	1.2 - 0.8	0.105
0.3	1.2 - 0.8	0.110
0.5	1.2 - 0.8	0.117
0.1	1.2	0.110
0.3	1.2	0.118
0.5	1.2	0.125

of the bipolaron and Ti^{3+} absorption bands might have influenced the evaluation of the Ti^{3+} ionization energy. It has to be noted, however, that in the case of bipolaron dissociation an increase of the 760 nm absorption was observed at 122 K already,¹⁸ as compared to ~ 250 K in the present case. Furthermore the decrease of the 580 nm Ti^{3+} band was found to be much weaker than that found previously for the 500 nm bipolaron absorption. With these arguments the presence of bipolarons can be excluded in the present case. This might be caused by the fact that the Ti^{3+} levels are somewhat lower than those of the bipolarons. The error limits of both electron stabilization energies allow for this possibility.

A slight temperature induced decrease of the Ti^{3+} absorption already starts at 10 K, but an accompanying increase of Nb^{4+} cannot be surely ascertained. If this is not the case, energy levels of other states between those of $Ti^{4+/3+}$ and $Nb^{5+/4+}$ have to be postulated. Such intermediate states will not, however, affect the determination of the Ti^{3+} ionization energy.

VI. SUMMARY AND OUTLOOK

We have investigated electron paramagnetic resonance of Ti^{3+} centers in reduced $LiTaO_3$ crystals. This new axial-symmetric defect center is analogous to the corresponding one in $LiNbO_3$ which was reported a few years ago. If interpreted on the basis of the theory of Abragam and Bleaney, both centers show unusually small orbital reduction parameters $k < 0.6$. We introduced a dynamic pseudo Jahn-Teller mechanism in order to explain the observed EPR signals, since covalency alone cannot account for such small k values. Different from related investigations of Bates *et al.* and Macfarlane *et al.* we avoid a perturbation treatment, because the relevant contributions to the Hamiltonian (i.e., spin-orbit coupling, trigonal crystal field, vibrational, and Jahn-Teller terms) are essentially of the same order of magnitude. Since a correspondingly full treatment, on the other hand, allows one to include only a finite number of interacting phonons, our results should be interpreted as a qualitative indication for essential vibronic couplings.

The second part of our investigations concerned the optical absorption of reduced Ti-doped $LiNbO_3$ crystals. At low temperatures the absorption spectrum shows a broadband peaked at 580 nm. Previously, ODMR in-

dicated that this band is related to Ti^{3+} ions. Upon heating this 580 nm band decreases in favor of a new absorption band at 760 nm which may be ascribed to Nb_{Li}^{4+} small bound polarons. The corresponding inter-valence transfer has been further studied by monitoring changes in the optical absorption intensities as a function of temperature. This allowed us to determine the energy separation between the $Ti^{4+/3+}$ and $Nb^{5+/4+}$ levels. The corresponding value of 0.11 eV turned out to be rather insensitive to the assumed initial defect concentrations. The existence of bipolarons which can principally affect our results could be excluded in our crystals on the basis of their qualitative different dissociation behavior.

Up to now we have investigated only moderately Ti-doped crystal samples. In order to get some further information concerning waveguides it is useful to consider reduced highly Ti-doped $LiNbO_3$. Here, we only report some preliminary results: First, we observe a change of the bulk Ti^{3+} EPR. The signal becomes more asymmetrical at the low field side and shifts to larger g values. This outcome may be caused by an overlap of two Ti^{3+} centers having slightly different g tensors. Second, we have identified a further Ti^{3+} EPR signal in reduced $LiNbO_3$ waveguides produced by indiffusion of Ti. This new EPR spectrum is related to a milky surface layer due to an unfinished indiffusion process. Indeed, the EPR signal decreases upon grinding away the surface layer. The symmetry of the new center is orthorhombic. For $\mathbf{B} \parallel \mathbf{c}$ we have measured $g_{\parallel} = 1.975 \pm 0.002$; for $\mathbf{B} \perp \mathbf{c}$ g varies between the extreme values $g_{\perp 1} = 1.974 \pm 0.002$ and $g_{\perp 2} = 1.939 \pm 0.002$ along directions perpendicular to each other. By comparison with g values identified for Ti^{3+} in TiO_2 ,²⁷ we are sure that we have identified Ti^{3+} possibly in a rutilelike environment. Rice *et al.*²⁸ suggested a corresponding intermediate crystal phase to occur during the Ti diffusion process.

ACKNOWLEDGMENTS

We wish to thank Dr. B. C. Grabmaier for kindly putting Ti-doped $LiNbO_3$ crystals at our disposal and T. Dollinger and W. Koslowski for expert assistance. We are grateful to H. Müller, who has performed the EPR measurement of $LiTaO_3:Ti^{3+}$. The research was supported by DFG, Sonderforschungsbereich 225.

¹ S. Juppe and O. F. Schirmer, *Phys. Lett. A* **117**, 150 (1986).

² H. Müller and O. F. Schirmer, *Radiat. Eff. and Defects Solids* **119-121**, 693 (1991).

³ A. Räuber, in *Current Topics in Material Science*, edited by E. Kaldis (North-Holland, Amsterdam, 1978), Vol. 1, p. 481.

⁴ C. Zaldo, C. Prieto, H. Dexpert, and P. Fessler, *J. Phys. Condens. Matter* **3**, 4135 (1991).

⁵ A. Abragam and B. Bleaney, *Electron Paramagnetic Resonance of Transition Ions* (Oxford University Press, New York, 1970), p. 417.

⁶ K. W. Blazey and K. A. Müller, *J. Phys. C* **16**, 5491 (1983).

⁷ R. M. Macfarlane, J. Y. Wong, and M. D. Sturge *Phys. Rev.* **166**, 250 (1968).

⁸ F. S. Ham, W. M. Schwarz, and M. C. M. O'Brien, *Phys. Rev.* **185**, 548 (1969).

⁹ C. A. Bates and J. P. Bentley, *J. Phys. C* **2**, 1947 (1969).

¹⁰ T. Kato, *Prog. Theor. Phys.* **4**, 514 (1949).

¹¹ T. Kato, *Prog. Theor. Phys.* **5**, 95 (1950).

¹² Although it is possible to prove, by additional considerations using Kato's perturbation theory (Refs. 10 and 11), that the above-mentioned perturbation problem belongs to

- the analytic branch of perturbation theory (i.e., the H_0 boundedness of the perturbations yields the energy as well as the state vector as analytic functions of the coupling coefficient), the coupling coefficients for Ti^{3+} in LiNbO_3 , LiTaO_3 , and Al_2O_3 turn out to be close to the limits of the convergence circle. Thus, convergence of a perturbation series might be poor.
- ¹³ R. Rai, *Phys. Status Solidi. B* **52**, 671 (1972).
- ¹⁴ M. H. L. Pryce, K. P. Sinka, and Y. Tanabe, *Mol. Phys.* **9**, 33 (1965).
- ¹⁵ G. F. Koster, J. O. Dimmock, R. G. Wheeler, and H. Statz, *Properties of the Thirty-Two Point Groups* (M.I.T. Press, Cambridge, MA, 1963).
- ¹⁶ M. Nippus, Ph.D. thesis, University of München, 1977.
- ¹⁷ H. Müller and O. F. Schirmer, *Ferroelectrics*, **125**, 319 (1992).
- ¹⁸ J. Koppitz, O. F. Schirmer, and A. I. Kuznetsov, *Europhys. Lett.* **4**, 1055 (1987).
- ¹⁹ J. M. Spaeth and F. Lohse, *J. Phys. Chem. Solids* **51**, 861 (1990).
- ²⁰ O. Thiemann, H. J. Reyher, and O. F. Schirmer, *Radiat. Eff. Defects Solids*. **119-121**, 571 (1991).
- ²¹ K. L. Sweeney and L. E. Halliburton, *Appl. Phys. Lett.* **43**, 336 (1983).
- ²² D. A. Dutt, F. J. Feigl, and G. G. DeLeo, *J. Phys. Chem. Solids* **51**, 407 (1990).
- ²³ O. Thiemann and O. F. Schirmer, *SPIE* **1018**, 18 (1988).
- ²⁴ S. C. Abrahams and P. Marsh, *Acta Crystallogr. B* **42**, 61 (1986).
- ²⁵ O. F. Schirmer, O. Thiemann, and M. Wöhlecke, *J. Phys. Chem. Solids* **52**, 185 (1991).
- ²⁶ H. Donnerberg, S. M. Tomlinson, C. R. A. Catlow, and O. F. Schirmer, *Phys. Rev. B* **40**, 11909 (1989).
- ²⁷ W. Low and E. L. Offenbacher, in *Advances in Research and Applications*, edited by F. Seitz and D. Turnbull (Academic Press, New York, 1965), Vol. 17, p. 135.
- ²⁸ C. E. Rice and R. J. Holmes, *J. Appl. Phys.* **60**, 3836 (1986).